Optimal Black Start Allocation for Power System Restoration

Georgios Patsakis, *Student Member IEEE,* Deepak Rajan, Ignacio Aravena, *Student Member IEEE,* Jennifer Rios, and Shmuel Oren, *Life Fellow, IEEE*

Abstract—Equipment failures, operator errors, natural disasters and cyber-attacks can and have caused extended blackouts of the electric grid. Even though such events are rare, preparedness for them is critical because extended power outages endanger human lives, compromise national security, or result in economic losses of billions of dollars. Since most of the generating units cannot restart without connecting to an energized grid, the system operator relies on a few units with the ability to start autonomously, called Black Start (BS) units, to restore the power system. Allocating and maintaining these units is costly and can severely impact the restoration security and time. We formulate an optimization problem to optimally allocate BS units in the grid, while simultaneously optimizing over the restoration sequence. We extend existing optimal allocation models by including grid considerations such as active power nodal balance, transmission switching, nodal reactive power support and voltage limits. In order to aid the branch and bound tree that solves the resulting large scale Mixed Integer Program (MIP), we propose a randomized heuristic that is executed multiple times in parallel on a high-performance computing environment to find feasible solutions. We proceed to solve the IEEE-39, the IEEE-118 and a simplified WECC system with 225 nodes and 136 generators to near optimality.

Index Terms—Black Start Allocation, Power System Restoration, Mixed Integer Programming, NERC Compliance

NOMENCLATURE

SETS

N	Set of buses.
E	Set of branches (ordered pairs of buses).
G	Set of generators.
$G(i)$	Set of generators connected to bus $i \in N$.
T	Set of consecutive integer time instances, starting from $1 \in T$.

VARIABLES

δ_i^t	Voltage phase of bus $i \in N$ at time $t \in T$.
f_{ij}^t	Network flow for energizing paths for branch $(ij) \in E$ at time $t \in T$.
f_g^t	Network flow for energizing paths from generator $g \in G$ at time $t \in T$.
$p_{SH_i}^t$	Active power load shed at bus $i \in N$ and time $t \in T$.

Georgios Patsakis and Shmuel Oren are with the Department of Industrial Engineering and Operations Research, and the Tsinghua-Berkeley Shenzhen Institute, University of California Berkeley. e-mail: gpatsakis@berkeley.edu

Deepak Rajan is with the Lawrence Livermore National Laboratory, California.

Ignacio Aravena is with the Center for Operations Research and Econometrics, UC Louvain, Belgium.

Jennifer Rios is with the Pacific Gas and Electric Company (PG&E), California.

p_g^t	Active power generation of generator $g \in G$ at time $t \in T$.
p_{ij}^t, q_{ij}^t	Active/reactive power flow of branch $(ij) \in E$ at time $t \in T$.
u_{BS_g}	Binary variable indicating generator $g \in G$ is a BS generator.
u_g^t, u_i^t, u_{ij}^t	Binary variable indicating generator $g \in G$, bus $i \in N$, branch $(ij) \in E$ energized at time $t \in T$ (zero indicates not energized).
v_i^t	Voltage magnitude of bus $i \in N$ at time $t \in T$.

PARAMETERS

$\underline{\delta}, \overline{\delta}$	Lower/upper bounds for voltage phases.
ϵ	Trade-off coefficient for line energization.
μ	Trade-off coefficient for inertia.
B	Total budget for BS generator installations.
$B_{SH_{ij}}$	Shunt susceptance of branch $(ij) \in E$.
b_{ij}, g_{ij}	Susceptance/conductance for branch $(ij) \in E$.
C_{BS_g}	Cost of turning $g \in G$ to a BS generator.
C_i	Cost of load shed in bus $i \in N$.
$\cos(\phi_{D_i})$	Power factor of load at bus $i \in N$.
J_g	Inertia of generator $g \in G$.
K_{R_g}	Ramping rate of generator $g \in G$.
P_{CR_g}	Cranking power required to be provided to generator $g \in G$ to initiate its start-up.
$\underline{P}_g, \overline{P}_g$	Minimum and maximum active power generation from generator $g \in G$ after the decomposition.
$P_g^{\min}, P_g^{\max}$	Minimum and maximum active power generation from generator $g \in G$ before the decomposition.
P_{D_i}	Available load at bus $i \in N$.
p_g^0	Initial active power of generator $g \in G$.
$\underline{Q}_g$	Minimum reactive power generation from generator $g \in G$.
Q_{SH_i}	Shunt reactor for bus $i \in N$.
$\overline{S}_{ij}$	Maximum flow limit for branch $(ij) \in E$.
T_{CR_g}	Time between generator $g \in G$ being energized until it can increase its active power from zero.
T_{CRIT_g}	Maximum critical time for generator $g \in G$.
u_g^0, u_i^0, u_{ij}^0	Binary parameter indicating the initial state of generator $g \in G$, bus $i \in N$, branch $(ij) \in E$.
$\underline{V}, \overline{V}$	Lower/upper bounds for voltage magnitude.

I. INTRODUCTION

On August 24, 2003 a fault of a high-voltage power line in Ohio initiated an extended blackout that affected 50 million

people for up to two days. The blackout contributed to at least 11 deaths and its cost was estimated at $6 billion. On September 8, 2011 an operator error caused an outage in California and Arizona that deprived 2.7 million people of electricity for up to 12 hours [1]. Natural phenomena, like earthquakes and wind storms, are also usual causes of extended outages; just in 2017 there have been multiple incidents nationwide (3.8 million customers without power due to Hurricane Irma in Florida in September, $800,000$ customers due to a wind storm in Michigan in March, $500,000$ homes in California in March). Recently, cyber attacks on the grid have been added to the concerns for a blackout, after hackers caused $225,000$ customers to lose power on December 23, 2015, in Ukraine. The North American Electric Reliability Corporation (NERC) and the Electricity Information Sharing and Analysis Center (E-ISAC) have worked to analyze the attack [2] and a lot of research is currently focused on the cyber-security of the power grid. However, in the event where counter measures fail, we need to restore the grid as fast as possible; especially since a hostile attack will try to take advantage of the moments after an outage where security is compromised.

The process of restoring the system back to normal operation involves crucial steps and considerations [3], [4]. Most of the generating units of the grid do not have the ability to restart by themselves, i.e. unless there is already an existing energized grid to connect to. For that reason, the system operators rely on a few units, called Black Start (BS) units, that can start independently. Clearly, the location and technical specifications of these units will directly affect the restoration time and security of the power grid. However, engaging a new generator as a BS unit is costly (in the order of millions of dollars) and is also associated with regular maintenance and testing costs (in the order of hundreds thousands of dollars) [5]. The Electric Reliability Council of Texas (ERCOT) has a biennial BS procurement process that typically procures 14-18 units [6]. The California Independent System Operator (CAISO) recently (May 2017) [7] identified a need for immediately procuring additional BS resources. So far there is no concrete optimization problem utilized to aid the process. The optimal allocation of BS units in the grid is the primary purpose of this paper.

The main considerations checked by the operators during the restoration process are: restoring critical loads as fast as possible, building paths to energize the non BS units, while maintaining frequency stability and avoiding voltage violations. The power systems restoration optimization problem, that incorporates the aforementioned concerns to generate valid restoration sequences, has received some attention recently. In [8], [9], the authors propose a step-wise strategy based on achieving specific milestones in the restoration process. In [10] an optimization problem that includes the generator active power capabilities is considered. However, the grid power flows are neglected and reactive power compensation, which constitutes a major concern for restoration, is not included. In [11] an aggregate reactive power constraint is utilized, but the grid flows are not. These considerations are addressed afterwards through heuristic modifications of the resulting sequence, however the changes undermine the

optimality of the final solution. A different modeling approach that includes reactive power considerations is adopted in [12], aiming to motivate the use of microgrids for the BS procedure, which is applied at a 6-bus system. A mixed integer non linear program is formulated in [13] and is heuristically solved using Ant Colony Optimization. Instead of the complete restoration, the sectionalization problem is solved in [14] using binary decision diagrams. An effort to integrate wind power in restoration is made in [15]. Literature reviews of relevant approaches are provided in [16], [17].

Even though the optimization of the restoration sequence is an interesting problem by itself, the need for restoration is a rare event in which the operators expect to base the restoration steps on their experience rather than software output not tested against actual restoration events. However, the allocation and contracting of BS units is a process that usually happens yearly for every operator, so the decisions associated with preparedness for the rare extended outages constitute an important problem that needs to be solved on a regular basis, even if the actual outage rarely occurs. General guidelines and methodologies for selecting BS units exist both in literature [18]–[20] and in restoration manuals [21]. There is limited research, however, on formulating an optimization problem to address the allocation. Recently, in [22], a minimum cost BS procurement problem was formulated, without considering the restoration sequence. In [23] the allocation optimization problem is enhanced by considering active power considerations of the restoration sequence, but not thermal line limits or reactive power compensation.

In our work, we formulate and solve the BS allocation problem, while also introducing innovations to the modeling of the restoration sequence formulation. The main contributions of this work are the following:

1) We introduce a new modeling approach utilizing one energization binary variable for every time step and one BS allocation binary variable to capture the widely used capability curves for BS and non BS generating units by decomposing them into two parts, which allows us to formulate the allocation problem in combination with the corresponding power system restoration problem.

2) We solve a BS allocation problem with a more detailed modeling of the restoration process than existing BS allocation literature, which is achieved by including constraints on the thermal limits of lines for the steps of the restoration sequence (by employing an approximation for the active and reactive power flows), constraints to alleviate overvoltage (through manipulation of active power flows, reactive power compensation or de-energization of transmission lines), and constraints that ensure the consistency of the grid at every step (allowing de-energization of transmission lines to alleviate overvoltages).

3) Due to the size and structure of the resulting optimization problem, commercial solvers encounter difficulties in identifying feasible solutions to it. For that purpose, we propose a randomized heuristic that is guided by linear programming (LP) relaxations to generate feasible solutions to the optimization problem and aid the

solvers.

The energization sequences generated by the optimization problem are checked for ac feasibility in the final step, as in [11], [24]. However, since most of the considerations have already been integrated in the optimization, the changes necessary to achieve ac feasibility are minimal.

The rest of the paper is organized as follows. In section II, the main concerns of the Power System Restoration Process are mentioned. In Section III, the proposed model constraints and objective are outlined. In Section IV the proposed heuristic is outlined, and simulation results for three test cases, the IEEE-39, the IEEE-118, and a simplified WECC system are presented.

II. POWER SYSTEMS RESTORATION

The restoration planning for most systems consists of constructing a plan that incorporates the priorities of the operators to ensure a secure system revival. Usually this plan is associated with the worst-case scenario, i.e. restoration from full blackout. In this section, we go through the basic considerations of the restoration process. Later, we present an optimization model that integrates most of these concerns.

A. System Identification and Preparation

The first step after a major outage is identifying and assessing the stability and safety of the remaining grid (if any), mitigating equipment and rating issues (voltage and thermal limits for the stable islands), and identifying equipment availability in order to build a restoration plan. Our ability to assess the system state can vary with the design of the protection system, SCADA penetration on both the transmission and distribution systems, and visibility of data, because of the disturbance. Most breakers of the transmission system are (remotely or manually) opened and the distribution is disconnected. Usually, the renewables are also disconnected, due to their intermittency.

B. Setting Priorities

The strategy for system restoration, whether from a BS resource or from a surviving island, is based on priorities that are dictated by reliability standards and are usually specific to the utility. For example, NERC Reliability Standard EOP-005-2 has identified restoration of off-site power to nuclear power plants as a priority of restoration. Providing power for auxiliary loads in order to energize non BS generating plants, restoration of fast starting units, station service batteries, control centers, major transmission lines, and restoration of stabilizing loads are all restoration priorities to technically support voltage and frequency of the grid during restoration. The ultimate restoration goal is to return the grid to normal operations (e.g. eliminate islands, restore inter-ties and customer load) quickly without compromising safety and reliably.

C. Reactive Power and Voltage Limits

Energizing transmission lines when served load is low (common during the restoration process) yields Ferranti rise considerations. More specifically, the capacitances of high voltage transmission lines inject reactive power into the system which leads to overvoltages in the endpoints of the energized transmission system, since loads that could induce an opposing voltage drop are not served. Reactive power compensation, to prevent limit violations, is achieved through shunt reactors or other VAR compensation connected to high voltage transmission lines, or synchronous generators that can absorb reactive power after being energized. In addition, grid operators engage in a few standard practices throughout the restoration process in order to keep voltages under check: picking up load with lagging power factor or de-energizing transmission lines.

D. Active Power and Frequency Regulation

Active power balance for all the islands is important during restoration to ensure the frequency remains within tolerances throughout the process. Frequency stability is directly influenced by the inertia of energized generators. In order to energize more generators, load must be picked up to ensure the generating units can ramp up (especially when technical minima of units must be satisfied). Loads with rotating masses, such as induction machines, may also be preferred during the restoration process for the same reasons.

III. OPTIMIZATION MODEL

As already mentioned, a BS unit has the ability to start on its own, without being connected into the grid. After a blackout, the BS units are responsible for partly energizing the grid by also providing cranking power to the units that do not possess BS capability. We represent the allocation of BS units using binary decision variables u_{BS_g}, for every generator $g \in G$. The typical way to achieve that is to install a smaller (often diesel) unit that will provide the cranking power. Generators that are already BS units can have a preassigned binary value of 1. If a generator cannot be chosen as a BS unit due to technical considerations, the binary variable is a priori set to zero. The restoration process is signified through binary variables for the various grid components (buses, lines and generators). A value of 1 indicates an energized component. In what follows, we describe the physical constraints and the objective for the BS allocation problem.

A. BS Allocation Budget Constraint

Costs are assigned for utilizing each one of the generating units as a BS resource. These costs could be set by the system operator (for example, ISO New England offers specific tariffs based on the ratings of generators [5]) or could be the bid of a generator after a call from the operator. The cost reflects not only the dedicated, usually diesel, generating unit used to restart the generator, but also the costs of testing and preserving the capability. For the purposes of modeling, we assume that the annual payments for BS services are converted into a one time capital cost:

$$\sum_{g \in G} C_{BS_g} u_{BS_g} \leq B \qquad (1)$$

B. Bus Active Power Balance

The bus balancing constraint has the form:

$$\sum_{j:(ji)\in E} p_{ji}^t + \sum_{g\in G(i)} \left(p_g^t + P_{CR_g}(u_{BS_g} - u_g^t)\right)$$
$$- \sum_{j:(ij)\in E} p_{ij}^t = P_{D_i} - p_{SH_i}^t, \forall i \in N, \forall t \in T \quad (2)$$

Constraint (2) stipulates the active power conservation at bus $i \in N$ every time instant $t \in T$. If a generator is chosen to be BS ($u_{BS_g} = 1$), then its cranking power is provided for (by an external source), so it can be immediately energized ($u_g^t = 1$). However, if we want a non BS generator g to be energized, the constraint introduces a negative term $-P_{CR_g}$, so the cranking power needs to be provided for either by a different generator or by flows into the bus. In the initial phases of the restoration, this constraint will ensure that only the generators that are assigned to be BS can actually be energized (i.e. have $u_g^t = 1$).

The load is modeled through a shedding variable that is equal to the total load in the case the bus is not energized:

$$(1 - u_i^t)P_{D_i} \le p_{SH_i}^t \le P_{D_i}, \forall i \in N, \forall t \in T \quad (3)$$

We note that it is not easy to know the maximum load P_{D_i} of a bus. When load is picked up after an outage, the demand is often greater than before, a phenomenon known as cold load pickup [25]. However, during restoration load is used as a controlable tool to accommodate voltage limits, ensure stable operation of the islands, or satisfy the minimum active power requirements of generators, so its actual maximum value is not central. We are also usually capable to pick it up in small chunks, so we assume a continuous load shedding variable, that can move between zero and maximum value; similar to the approach in [24]. The model currently has no constraints for the rate of load pickup. In the power systems restoration literature, the problem of restoring the load is often solved after the restoration sequence is acquired [26], [27], so that more detailed load pickup models can be used. Frequency stability issues become important when the actual load pickup actions are considered [28], [29].

C. Bus Reactive Power Constraint

Reactive power capacity is important in maintaining the voltages of the power system within reasonable limits. Since the main concern during the restoration process is the capability of the system to absorb the reactive power generated by the high capacitance of the lines, we only consider a single directional constraint approximating the capability of the system units to absorb reactive power. The following constraint is introduced at every bus:

$$\sum_{j:(ji)\in E} q_{ji}^t - \sum_{j:(ij)\in E} q_{ij}^t + \sum_{g\in G(i)} \underline{Q}_g u_g^{\max\{0, t-T_{CR_g}-1\}}$$
$$+ \sum_{j:(ji)\in E} \frac{1}{2}B_{SH_{ji}} u_{ij}^t + \sum_{j:(ij)\in E} \frac{1}{2}B_{SH_{ij}} u_{ij}^t + Q_{SHi} u_i^t \quad (4)$$
$$\le (P_{D_i} - p_{SH_i}^t)\tan(\phi_{D_i}), \forall i \in N, \forall t \in T$$

A line injects reactive power $\frac{1}{2}B_{SH_{ij}} V^2 u_{ij}^t$ at each of the buses it connects to, if energized, where the bus voltage V is

assumed close to one for this constraint, to allow for a linear formulation. The reactive power can be absorbed by either generators that have been energized at least $T_{CR_g}+1$ time units in advance, or by reactive compensation connected to the bus Q_{SH_i}, or by loads with lagging power factor ($\tan(\phi_{D_i}) > 0$). The load is assumed picked up at a constant power factor, as in [24] and [12]. While not a precise approximation, the reactive power constraints ensure that: (i) Every island formed during the restoration process has adequate reactive power absorption capability. To see why this is true, one can add all of the equations (4) for the nodes of an island that may arise in the restoration process. The reactive flows that lead outside the island are set to zero by (7). The reactive flows that are within the island cancel each other. What remains is the constraint that the total (aggregate) reactive power absorption capacity of the island exceeds the total reactive power injection by the lines. (ii) There is no reactive power sink (i.e. the reactive power generated by transmission lines must be absorbed by some component of the system). The equations may allow for fictitious reactive power generation, but this is an inferior concern for restoration, since the system typically operates under excessive reactive power generation.

D. Generator Model

A typical generator startup curve is assumed, as in [10], [11], see Fig. 1. The curve is decomposed into two parts, as shown in 1. The binary variable u_g^t is associated with the energization state of generator $g \in G$ (i.e. it is 1 for $t \ge t_{start}$). This variable is exogenously defined based on the availability of active power or BS unit assignment in (2). That requirement corresponds to Fig. 1c. The modeling of the generator output in Fig. 1b will now be defined based on the following constraints:

$$0 \le p_g^\tau \le \overline{P}_g u_g^t, \forall g \in G, \forall \tau \in \{t, t+1, \dots, t+T_{CR_g}+1\},$$
$$\forall t \in T \cup \{0\} \quad (5a)$$
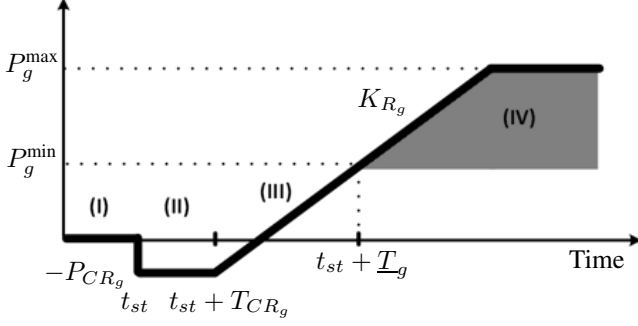$$p_g^t - p_g^{t-1} \le K_{R_g}, \forall g \in G, \forall t \in T \quad (5b)$$
$$p_g^{t-1} - p_g^t \le K_{R_g}, \forall g \in G, \forall t \in T \quad (5c)$$

Constraint (5a) makes sure that the active power can not become positive for at least T_{CR_g} units of time after the generator is energized, both for BS and for NBS generators. Also, the maximum active power limit is imposed at all time instances that the generator has positive active power production. The ramping rate capability is imposed through the constraints (5b) and (5c). Next, the following constraint for a generator $g \in G$ would ensure that the minimum active power generation limit $\underline{P}_g$ is satisfied, after the cranking time has passed and the generator has ramped up to $\underline{P}_g$.
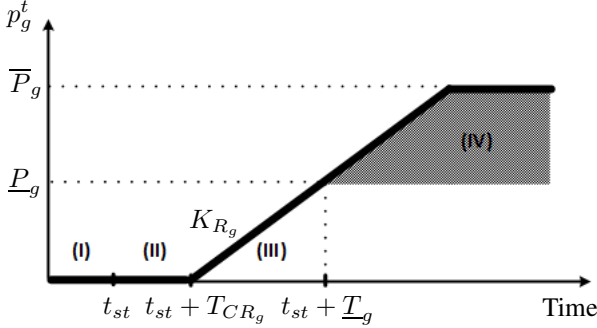
$$p_g^\tau \ge \underline{P}_g u_g^t, \ \forall\, \tau \ \ge (t + T_{CR_g} + \underline{P}_g/K_{R_g}), \forall t \in T \quad (6)$$
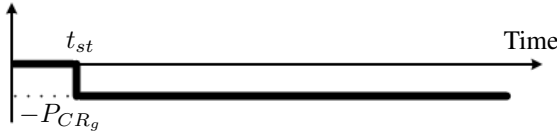
E. Line Switching

In order to model the formation of islands, a constraint that stipulates that active and reactive flows can only go through lines that are energized needs to be enforced. For that purpose, the ideas from transmission switching [30] are utilized, with a modification to accommodate for reactive power. The same

(a) A disconnected generator $g \in G$ (phase I) gets energized at time t_{st} (i.e. u_g^t becomes 1 at $t = t_{st}$) and needs to be cranked for a period of T_{CR_g} (phase II). During the cranking period, the generator absorbs the cranking power P_{CR_g} (negative generation). The generator then starts to ramp up to its technical minimum $\underline{P}_g$ (phase III) at time $t_{st} + \underline{T}_g$, where $\underline{T}_g = T_{CR_g} + (P_{CR_g} + P_g^{min})/K_{R_g}$. Afterwards, generation can freely move between P_g^{min} and P_g^{max}, within the ramping capability K_{R_g}. This model appears in other works, such as in [8] and [11]. For the purposes of this work, we decompose the model as the superposition of the two curves below.

(b) The first part of the decomposed generator model. The generation levels in the graph are defined as $\underline{P}_g = P_g^{min} + P_{CR_g}$ and $\overline{P}_g = P_g^{max} + P_{CR_g}$.

(c) The second part of the decomposed generator model. This is essentially a negative step function to the cranking power of the generating unit at the time of energization ($u_g^t = 1$). The allocation of the BS units allows for u_g^t to become 1, even if there is no external power fed to the unit.

Fig. 1: Typical generator active power curve and its decomposition into two parts. The parameters $T_{CR_g}, \underline{T}_g, P_{CR_g}, K_{R_g}, \underline{P}_g, \overline{P}_g$ vary depending on the type of generator.

ideas have been utilized in other works on restoration and islanding as well [31].

$$|p_{ij}^t| + |q_{ij}^t| \le u_{ij}^t \overline{S}_{ij}, \forall (ij) \in E, \forall t \in T \tag{7}$$

Constraint (7) is an approximation of the constraint $\sqrt{(p_{ij}^t)^2 + (q_{ij}^t)^2} \le u_{ij}^t \overline{S}_{ij}$ in the following way: if the line is not energized, both equations set its active and reactive power flow to zero. If the line is energized, an apparent power limit is imposed on the line. Due to the inequality $\sqrt{(p_{ij}^t)^2 + (q_{ij}^t)^2} \le |p_{ij}^t| + |q_{ij}^t|$, constraint (7) is tighter than the physical limit (L-1 ball instead of the L-2 ball with the same radius). The two constraints are in disagreement mainly in the area of simultaneously large values of both

active and reactive flow, a setting that we rarely expect to occur during the initial steps of restoration (the load is at most 10-20% restored by the end of the time horizon we are considering). Constraint (7) is eventually substituted by four linear constraints to eliminate the absolute values.

$$p_{ij}^t = -b_{ij}(\delta_i^t - \delta_j^t)u_{ij}^t, \forall (ij) \in E, \forall t \in T \tag{8a}$$
$$q_{ij}^t = \left(-b_{ij}(v_i^t - v_j^t) - g_{ij}(\delta_i^t - \delta_j^t)\right)u_{ij}^t, \forall (ij) \in E, \forall t \in T \tag{8b}$$
$$\underline{\delta} \le \delta_i^t \le \overline{\delta}, \forall i \in N, \forall t \in T \tag{8c}$$
$$\underline{V} \le v_i^t \le \overline{V}, \forall i \in N, \forall t \in T \tag{8d}$$

Constraints (8a) and (8b) set the active and reactive power flow of line $(ij) \in E$ to zero, if the line is not energized ($u_{ij}^t = 0$), and impose a linearized approximation of the active and reactive power flows otherwise. Both line susceptances and conductances are considered for reactive power, since eliminating overvoltages during the restoration process is commonly performed not only through reactive power compensation, but also by picking up load to induce active flows. These equations are linearized via a big-M reformulation, as in [30], which combined with (7), yields the same feasible region as (8a) and (8b). For example, constraint (8a) yields:

$$b_{ij}(\delta_i^t - \delta_j^t) + p_{ij}^t \le (1 - u_{ij}^t)M_{ij}, \forall (ij) \in E, \forall t \in T \tag{9a}$$
$$b_{ij}(\delta_i^t - \delta_j^t) + p_{ij}^t \ge (u_{ij}^t - 1)M_{ij}, \forall (ij) \in E, \forall t \in T \tag{9b}$$

where $M_{ij} = |b_{ij}|(\overline{\delta} - \underline{\delta})$.

F. Consistency of energized grid

A series of constraints need to be imposed to ensure consistency of the grid at any given time point. More specifically, we need to enforce that all the energized buses of the grid at any time instant are connected to an energized generator through a path of energized lines.

$$0 \le f_g^t \le u_g^t, \forall g \in G, \forall t \in T \tag{10a}$$
$$-u_{ij}^t \le f_{ij}^t \le u_{ij}^t, \forall (ij) \in E, \forall t \in T \tag{10b}$$
$$\sum_{j:(ji)\in E} f_{ji}^t - \sum_{j:(ij)\in E} f_{ij}^t + \sum_{g\in G(i)} f_g^t = \frac{1}{N}u_i^t,$$
$$\forall i \in N, \forall t \in T \tag{10c}$$

(10a), (10b) and (10c) impose a feasibility problem given fixed values of u_g^t, u_{ij}^t and u_i^t for the flows f_{ij}^t and f_i^t. A bus can be energized ($u_i^t = 1$) if there is a feasible flow from one or more of the generators with $u_g^t = 1$, flowing only through branches with $u_{ij}^t = 1$, such that a fictitious load on that bus of $\frac{1}{N}u_i^t$ can be satisfied. Otherwise, the state of that bus has to be $u_i^t = 0$.

Additional constraints that ensure the consistency of the grid are also necessary. If a generator connected to a bus is energized, then the bus is considered energized:

$$u_g^t \le u_i^t, \forall i \in N, \forall g \in G(i), \forall t \in T \tag{11}$$

A line can get energized at a time step only if one of the buses connected to it was energized at the previous time step:

$$u_i^t \le u_i^{t-1} + u_j^{t-1}, \forall (ij) \in E, \forall t \in T \tag{12}$$

Also, when a branch gets energized, both of the buses connected to it are energized:

$$u_{ij}^t \leq u_i^t, u_{ij}^t \leq u_j^t \, , \forall (ij) \in E, \forall t \in T \qquad (13)$$

Finally, we assume that buses and generators are picked up only once:

$$u_g^t \geq u_g^{t-1} \, , \forall g \in G, \forall t \in T \qquad (14a)$$

$$u_i^t \geq u_i^{t-1} \, , \forall i \in N, \forall t \in T \qquad (14b)$$

Note the same assumption is not made for lines. The reason is that de-energizing lines is a standard practice included in the restoration guidelines that some grid operators have developed to alleviate overvoltages, so our modeling allows for such operating practice. Allowing line de-energization is what makes constraints (10a)-(10c) necessary in our formulation.

G. Optimization Objective

The objective of the problem in general will highly depend on the priorities set by the characteristics of each particular system. A generic form can be the following:

$$\min \sum_{t \in T} \left(\sum_{i \in N} C_i^t p_{SH_i}^t - \mu \sum_{g \in G} u_g^t J_g - \epsilon \sum_{(ij) \in E} u_{ij}^t \right) \qquad (15)$$

(15) penalizes the load shed (depending on the criticality of the load), incentivizes increasing the total inertia of the energized system, and encourages the complete energization of the grid. The final form of the objective ultimately depends on the priorities of the particular system; a vital load will carry high cost, or energizing a generating plant or government or industrial consumer will be considered more important.

IV. A HEURISTIC

We used a commercial solver (FICO Xpress Optimizer [32]) to handle the optimization problem formulated in the previous section. We observed that the solver struggled to find feasible solutions to the problem using its own heuristics, even when an increased number of threads was devoted to that purpose. For that reason, we developed a custom heuristic that utilizes the time-staging structure of the problem, is guided by LP relaxations and tries to identify feasible solutions. Randomization is used at various parts of the heuristic, so that multiple executions can yield different solutions. The solutions are then fed to the solver to aid the branch and bound tree. Multiple runs of the heuristic can be launched in parallel in a high performance computing environment to speed up the process. The heuristic consists of two phases. In the BS Allocation Phase, the BS units are assigned and the value of u_{BSg} is fixed to an integer for the next phase. In the Restoration Sequence Phase, the restoration sequence based on the BS units is fixed. Both phases use the function RANDOMRANK (given in Fig. 2), which takes a list of fractional values as input, perturbs them by noise (by adding αX, where X is uniformly distributed in $[0, 1]$ and α a controllable parameter that influences how much randomness will be injected in the LP relaxation solution), and returns a ranked list. We also allow the solver to tighten the relaxation by exploiting the integral nature of the variables.

1: **Black Start Allocation Phase**
2: $t \leftarrow 0$
3: Solve LP relaxation. Get $u_{BS_g}^{LP} \in [0, 1]$, $\forall g \in G$
4: Pick generators in order RANDOMRANK $(\{u_{BS_g}^{LP}\}_{g \in G}, \alpha_{BS})$ as BS (fix u_{BS_g} , $\forall g \in G$) up to budget B.
5: Based on fixing of BS, ramping rates and active and reactive power limitations, update active and reactive power capabilities of the generators $\forall t \in T$.
6: Initialize islands, generator and node labels corresponding to the BS units.
7: **Restoration Sequence Phase**
8: **for** $\tau \in T$ **do**
9:     Solve LP with u_{BS_g} and u_g^t, u_{ij}^t, u_i^t fixed for $t \leq (\tau - 1)$.
10:     **Line Selection**
11:     **repeat**
12:         Pick next line $(i', j') \in E$ based on RANDOMRANK $(\{u_{ij}^{\tau, LP}\}_{(ij) \in E}, \alpha_E)$ with $u_{i'j'}^{\tau, LP} > 0$
13:         **if** New Reactive Power Capability in Island of $(i', j') \geq R_Q$ **then**
14:             Add line (fix $u_{i'j'}^{\tau} = 1$) and corresponding nodes (fix $u_{i'}^{\tau} = 1$ or $u_{j'}^{\tau} = 1$) if necessary.
15:             Update islands
16:             Update node, line and generator labels.
17:         **end if**
18:     **until** all lines with $u_{i'j'}^{\tau, LP} > 0$ tested
19:     **Generator Selection**
20:     **repeat**
21:         Pick next generator $g' \in G$ based on RANDOMRANK $(\{u_g^{\tau, LP}\}_{g \in G}, \alpha_G)$ with $u_{g'}^{\tau, LP} > 0$ and connected to an energized node.
22:         **if** New Active Power Capability in Island of $g' \geq R_P$ **then**
23:             Add generator (fix $u_{g'}^{\tau} = 1$).
24:             Update generator labels.
25:             Based on ramping rate and active and reactive power limitations, update active and reactive power capability of $g' \, \forall t \in T$.
26:         **end if**
27:     **until** all connected generators with $u_{g'}^{LP} > 0$ tested
28: **end for**
29:
30: **function** RANDOMRANK $(\{u_k\}_{k \in K}, \alpha)$
31:     $r_k \leftarrow u_k + \alpha X_k$, where $X_k \sim$ Unif$(0, 1)$
32:     Rank elements of K based on r_k: Let $R : \{1, \ldots, |K|\} \mapsto K$ be a bijection s.t. $i > j \iff r_{R(i)} \leq r_{R(j)}$
33:     **return** R
34: **end function**

Fig. 2: Randomized Heuristic for feasible point search.

In the BS Allocation Phase, the LP relaxation of the full problem is solved. From the solution $(u_{BSg}^{LP} \in [0, 1])$, the generators are ranked (using RANDOMRANK with $\alpha = \alpha_{BS}$) and picked based on the ranking, up to the available budget B. For the rest of the heuristic the BS allocation is considered fixed, i.e. the binary decision variables u_{BSg} are fixed to integral values. The Restoration Sequence Phase adopts the following pattern: At every step τ in the time horizon an LP relaxation is solved. Then, based on the relaxed values obtained from the assignment variables of lines $u_{ij}^{\tau, LP}$ and generators $u_g^{\tau, LP}$ at this time step, all binary variables for time τ are fixed to integral values for the next steps, and the process is repeated. However, a simple randomized rounding scheme would not work because it is very easy to construct an infeasible combination. Instead, at every step we make intelligent fixings by tracking the islands that are formed, and labeling every bus, line and generator by the index of the island they belong to (unlabeled if not yet energized). This phase of the algorithm has two parts: the Line Selection part defines the topology, i.e. which lines and buses are going to be introduced, whereas the Generator Selection part defines

which generators will be energized.

In the Line Selection part, a ranking of the lines is again formed (using RANDOMRANK with $\alpha = \alpha_E$) based on the LP relaxation values. However, only lines with positive relaxation values $u_{ij}^{\tau,LP}$ are considered in the ranking, since these are guaranteed to be lines connected to at least one bus energized at the previous time step, due to constraint (12). Then, the lines are sequentially introduced according to their ranking. Since the main concern with energizing lines is the reactive power they inject into the system (which could cause overvoltage problems due to the Ferranti effect), the reactive power capability of the island that would be created if the line was connected is checked before deciding to introduce the line. At the same time, given that the constraint is only checked at an island level, a higher threshold R_Q may be used to possibly account for not considering the local effect for that line. In the Generator Selection phase, the LP relaxation again yields a ranking of the generators (using RANDOMRANK with $\alpha = \alpha_G$). A similar test is performed to qualify introducing the generator; in this case, the main concern is whether or not the island possesses adequate active power capacity to provide for the cranking power of the generator, plus some slack of R_P to accommodate for only checking this constraint on an island level. If the generator has a minimum stable operational limit $\underline{P}_g$, then the load capability of the island to accommodate for this generation is also tested.

V. EXPERIMENTAL RESULTS

All the simulations are performed on the Cab cluster of the Lawrence Livermore National Laboratory. The Cab cluster consists of 1296 nodes with 20736 cores, with an Intel Xeon E5-2670 processor at 2.6 GHz and 32 GB per node. For the simulations, Mosel 4.0.4 was used with Xpress [32]. The heuristic simulations were parallelized at 6 nodes by utilizing Mosel, with 4 jobs per node and 4 threads per job.

A. Simulation of the IEEE-39 Bus System

In order to illustrate the effectiveness of the proposed model, a small test case is initially considered. The IEEE-39 bus system consists of 39 buses, 10 generators and 34 branches [33]. The most important parameters for the problem are given in Table I; most of the cranking powers and cranking times for that system are taken from [11]. The parameters for generator 10 are purposefully chosen in a way that favors turning it into a BS unit (i.e. small cranking power of 1MW
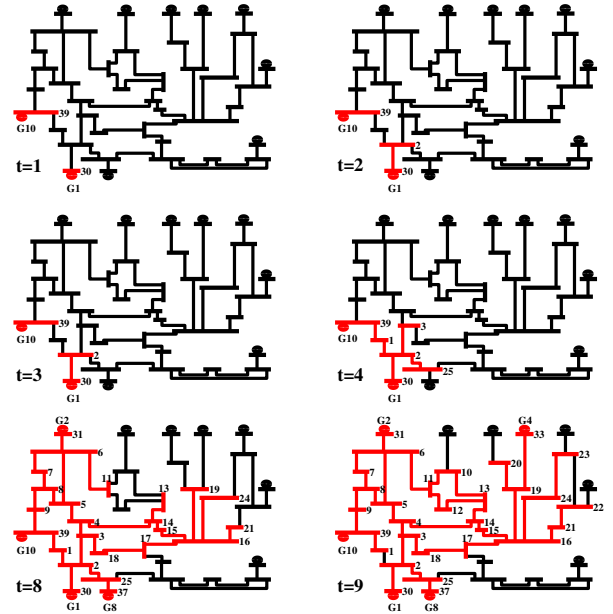

Fig. 3: Sampled steps of the restoration process. Generators 1 and 10 are chosen by the optimization problem as BS units, so they get energized first. The rest of the grid is gradually restored. The time unit is 5min. Note that the line connecting buses 2 and 30 is picked up immediately after energization, because it has no shunt capacitance in the model. However, the generators cannot pick further transmission lines immediately, since they can not change their reactive power setpoint up until one period after the cranking is over (i.e. after time 3 for G1). Notice also that the line connecting buses 1 and 39 gets de-energized at time $t = 9$. Forcing energization of the line at this time point leads to ac infeasibility, which means that the flexibility of de-energizing lines (enabled by the model) is utilized.
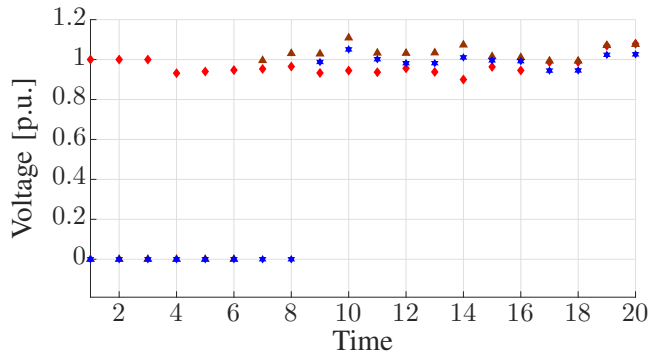

Fig. 4: Voltages of three buses from the ac simulations. Bus 16 (brown triangles) is on the edges of the transmission system and suffers from overvoltages (in fact at time $t = 10$ we need to relax the voltage limit to 1.12p.u. for one time step). Bus 30 (red diamonds) is a generator bus and its value is set as low as possible, to accomodate for reactive power transfer to the transmission system. Finally, the voltage of bus 20 is depicted with blue hexagrams. The transition from zero to nonzero values indicates the time step that a node is energized.

and a small cranking time of 10 minutes). The cost of load shedding at every bus is set to $(5000 + 50 * i)$\$/MWh, where i is the bus number of the load. Both μ and ϵ are set to comparatively small values (equal to 100). The length of the time horizon is set to $T = 40$ time units, with a 5 minutes time step. The problem has 36058 constraints and 16380 variables, of which 3810 are binary. Xpress struggles to find feasible solutions to the problem. After 30 minutes, only one feasible solution was found, with an optimality gap of 43.30%. Gurobi performs better for this small problem, by finding a solution
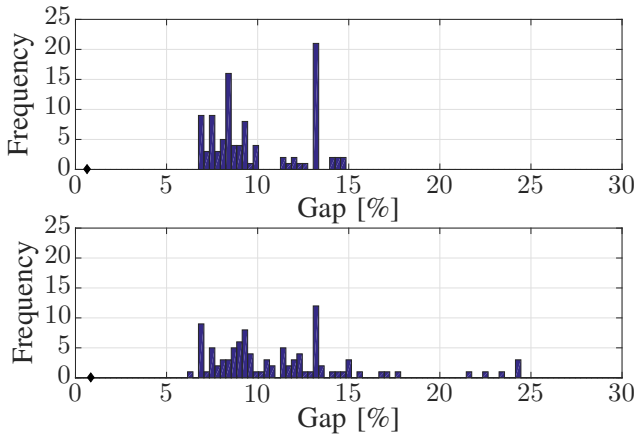
Unit	P_{CR_g} [MW]	$\underline{Q}_g$ [MVar]	K_{R_g} [MW/h]	C_{BS_g} $(B = 30)$
G1	6	−400	215	13.5
G2	8	−300	246	15.5
G3	7	−300	236	14.5
G4	5	0	198	12.5
G5	8	0	244	15.5
G6	6	−300	214	13.5
G7	6	0	210	13.5
G8	13	0	346	20.5
G9	15	−300	384	22.5
G10	1	−300	162	8.5

TABLE I: Data used for the IEEE-39 system. All the cranking times are set to $T_{CR_g} = 30$min, except $T_{CR_{10}} = 10$min.

Fig. 5: Gap for 100 feasible solutions generated by the heuristic, for two different settings of the value of α_{BS}, i.e. $\alpha_{BS} = 0$ (plot above) and $\alpha_{BS} = 1.5$ (plot below). The values of α_E and α_G are set to 0.5. The heuristic solutions were fed to the optimizer, which solved the problem within 1% tolerance. The gap for that solution is shown with a diamond on the plots. Increased randomness (meaning the heuristic moves randomly away from the LP relaxation solution) leads to worse feasible solutions in general, but may also get lucky and find a better feasible solution.

with 1% gap within 20 minutes.

As an alternative, we launch parallel heuristic executions in Xpress until 100 feasible solutions are found (which takes approximately 15 minutes). The feasible solutions are then fed to Xpress and the solver usually achieves the desired 1% gap within 15 minutes. The purpose of the heuristic is therefore not to completely substitute the optimization solver, but to guide it.

In the optimal allocation, generators 1 and 10 (as expected) are chosen. Generator 1 was selected due to its high reactive capability (which is important for that system that has no reactors for compensation). Some steps of the restoration process are presented in Fig. 3.

We also check the restoration sequence for ac feasibility. For that, an ac feasible point is sought for the grid configuration at every step and given the various unit capabilities, as in [11], [24]. The islands are identified at every step and an ac optimal power flow (OPF) is performed using the software Matpower [34]. The load is initially considered fixed at the value provided by the optimization problem. If this does not yield an feasible point, the load is perturbed by no more than 10% around that value. This was adequate for finding feasible points at all time instances, apart from three in which the upper voltage limit had to be relaxed from 1.1 to 1.12; see Fig. 4. A systematic way to perform this task is described in [26].

Finally, in Fig. 5, heuristic executions for two different settings of the parameter α_{BS} are shown. Note that none of the heuristic executions gets very close to the best integer solution found. This is due to the fact that the final integer allocation assigns a generator (G1) with a very small u_{BS_g} value in the LP relaxation, so the heuristic is unlikely to make this assignment. Furthermore, the heuristic by construction lacks some characteristics that the optimal solution could have, such as the ability to de-energize lines. Such modifications are left for the local search of the solvers to identify.

Parameters	Time for M feasible points [s]			
$(\alpha_{BS}, \alpha_E, \alpha_G)$	$M = 5$	$M = 50$	$M = 100$	$M = 1000$
$(0.8, 0.5, 0.5)$	218	791	1133	10045
$(0.8, 1.5, 0.5)$	242	688	1263	10656
$(0.8, 0.5, 1.5)$	228	653	1110	10808
$(0.8, 1.5, 1.5)$	236	701	1193	11304

TABLE II: Time for the heuristic to find the designated number of feasible solutions for the IEEE-118 system, depending on the randomness parameters. For many executions ($M = 1000$), increased randomness yields higher computational times, due to more points identified by the heuristic being infeasible; the difference is in general not observable for fewer executions.

B. Simulation of the IEEE-118 Bus System

The IEEE-118 bus system consists of 118 buses, 186 branches and 54 generators. The data from [35] were used for cranking powers, ramping rates and cranking times of the generating units. The allocation costs were assumed to have two parts: 70% of the cost was assumed the same for all units and the remaining 30% was assumed proportional to the BS unit's cranking power. The total budget is assumed 15% of the cost of assigning all the units as BS. For the 345kV lines, reactive compensation equal to approximately 45% of their capacitance was assumed connected to each of their endpoints (reactive compensation of this size appears in actual systems to alleviate the Ferranti rise). The cost of load shed was set in the same way as for the IEEE-39 bus system. A time resolution of 15 minutes was considered, for 20 time steps.

The optimization problem has 70704 constraints and 30028 variables, of which 7214 are binary. When the problem is fed to the Xpress Optimizer, the solver is unable to identify a feasible solution within a 5 hour time limit. Gurobi can only find the feasible solution corresponding to setting all binaries to zero (i.e. making no actions to restore the power system) within the same time limit. Executions of the heuristic identify feasible solutions, as well as eventually the optimal solution (verified by the solver due the the termination of the branch and bound tree search), and the performance with respect to time is depicted in Table II. Six generators are assigned as BS units (G21, G22, G25, G28, G45 and G51). In order to signify the importance of the voltage constraints, Fig. 6 indicates the buses at which voltages are set to their maximum or minimum limits from the optimization. The resulting solution is also tested for ac feasibility at every time step.

C. Simulation of the reduced WECC system

As a final test case, we consider a reduced model of the Western Electricity Coordinating Council (WECC) system [36] with 225 buses, 371 lines, 130 conventional generators and 6 hydro units. The same model is used in [37][1]. The generation mix in terms of type, number of generators and total capacity is shown in Table III. The renewable energy generation is assumed disconnected during the restoration, with the exception of hydro. The imports are also assumed disconnected. A time horizon of 18 steps with 15 minute resolution was considered.

[1]Data available at the following link: https://drive.google.com/drive/u/2/folders/1F3u6yq-noQhv8APZKaa45mM0q1I9_-cy.
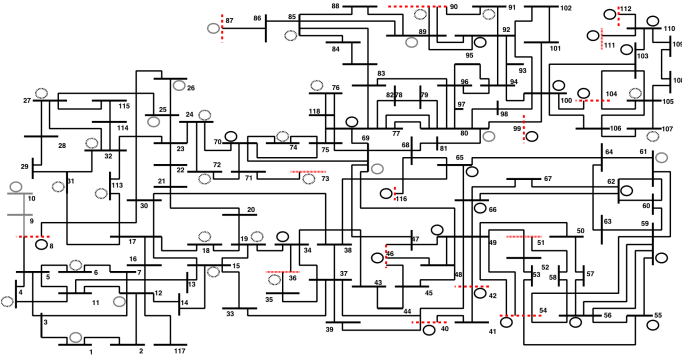
Fig. 6: Snapshot of the IEEE-118 system ($t = 10$). The non energized part is depicted in gray, generators with bold black line have nonzero output, whereas dotted generators are being cranked. Red dotted bus lines and red dashed bus lines indicate buses at their maximum and minimum voltage respectively. Note that buses of generators with reactive power support (such as 46) are usually set to the minimum voltage (in order to absorb reactive power), whereas some buses at the edges of transmission (such as 51) are set to the maximum.

Type	Units	Capacity [MW]
Nuclear	2	4499
Gas	101	21781
Coal / Oil	3 /1	199 / 121
Dual Fuel	23	4679
Hydro	6	8613

TABLE III: Generator mix for the WECC test system.

One of the crucial priorities when energizing the grid is providing power to the nuclear power plants, due to security considerations. For this reason, a penalty was associated in the objective with u_g^t for the nuclear power plants to ensure their quick restoration. The total budget is assumed 4% of the total cost for allocating all the units. Nuclear power plants are excluded from serving as black starts (by setting the corresponding binary allocation variable to zero).

The optimization problem has 131470 constraints and 55418 variables, of which 13597 are binary. Xpress and Gurobi were unable to find any feasible solutions within the 5 hour time limit imposed. The heuristic is launched and finds 20 feasible solutions within 40 minutes. The optimization problem is then solved within 6.7% optimality gap in Xpress, after 2 hours of execution. The power plants allocated were three hydro plants, which is expected due to their small cranking power and cranking time (they constitute ideal BS units), as well as one gas station at McCall. The gas station was allocated due to its proximity to the nuclear power plant at Diablo Canyon (since none of the hydro units are in the vicinity). The sequence was also tested for ac feasibility.

VI. CONCLUSIONS AND FUTURE RESEARCH

In this work, we formulated and solved the optimal BS allocation problem. We enhanced existing literature on the topic with a new modeling approach and sets of constraints to accommodate for some of the most important considerations during restoration. Based on our understanding of the problem structure, we proposed a heuristic guided by the LP relaxation of the optimization. The feasible solutions generated by the heuristic are then fed into commercial solvers, which can then
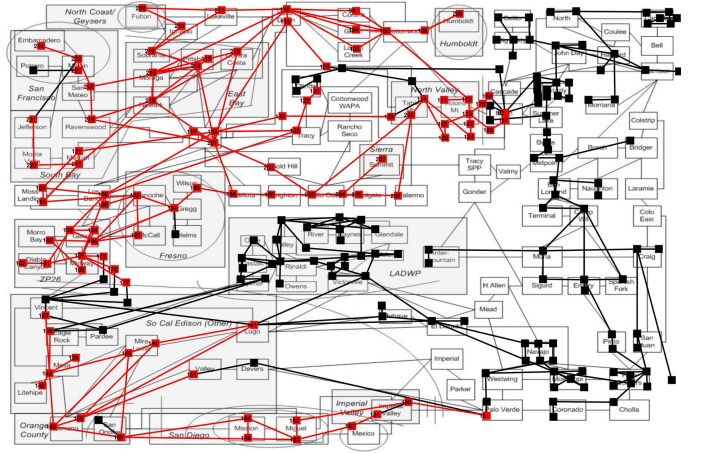

Fig. 7: Snapshot of the restoration for the WECC system (restored part in red).

provide global guarantees for optimality. Our subsequent goal, is to apply our model for simulating actual power systems. For such a setup, the heuristic should become even more useful, since it is based on solving LPs (the algorithms for which are considered mature and efficient even in the case of hundreds of thousands of variables and constraints) and it may be the case that the heuristic becomes the only approach. Tighter reformulations of the constraints of the problem can also be developed and the benefit from their use will be explored. Furthermore, since the initial state of the system (i.e. the stable islands after a blackout) is a parameter to our problem, a BS allocation that can accommodate for a number of scenarios can be achieved by solving a two-stage stochastic program. In this case, the first stage decision will be the BS allocation, the scenarios will be a number of possible outages (defined by experts), and the second stage will be the restoration steps according to the scenario. One final direction we wish to pursue is to see if we can extend our algorithmic approach to provide grid resiliency services by microgrids, as in [38], by allocating microgrids as BS resources.

REFERENCES

[1] Patrick J. Kiger, "Blackouts: A history," National Geographic: http://channel.nationalgeographic.com/american-blackout/articles/blackouts-a-history/, 2013, [Online; accessed Aug-2017].
[2] R. M. Lee, M. J. Assante, and T. Conway, "Analysis of the cyber attack on the Ukrainian power grid," *SANS Industrial Control Systems*, 2016.
[3] N. Fountas, N. Hatziargyriou, C. Orfanogiannis, and A. Tasoulis, "Interactive long-term simulation for power system restoration planning," *IEEE Transactions on Power Systems*, vol. 12, no. 1, pp. 61–68, 1997.
[4] S. Liu, Y. Hou, C.-C. Liu, and R. Podmore, "The healing touch: Tools and challenges for smart grid restoration," *IEEE power and energy magazine*, vol. 12, no. 1, pp. 54–63, 2014.

[5] ISO New England, "Schedule 16 - Blackstart standard rate report," https://www.iso-ne.com/isoexpress/web/reports/billing/-/tree/schedule-16---blackstart-standard-rate-report, 2016, [Online; accessed Aug-2017].

[6] S. Sharma, "ERCOT black start enhancements," Electric Reliability Council of Texas: http://www.ercot.com/content/wcm/key_documents_lists/108699/06._ERCOT_BlackStart_Enhancements.pptx, 2017, [Online; accessed Aug-2017].

[7] California ISO, "Black start and system restoration Phase 2," https://www.caiso.com/informed/Pages/StakeholderProcesses/Blackstart_SystemRestorationPhase2.aspx, 2017, [Online; accessed Aug-2017].

[8] Y. Hou, C. C. Liu, K. Sun, P. Zhang, S. Liu, and D. Mizumura, "Computation of milestones for decision support during system restoration," *IEEE Transactions on Power Systems*, vol. 26, no. 3, pp. 1399–1409, Aug 2011.

[9] S. Liu, R. Podmore, and Y. Hou, "System restoration navigator: A decision support tool for system restoration," in *Power and Energy Society General Meeting, 2012 IEEE*. IEEE, 2012, pp. 1–5.

[10] W. Sun, C.-C. Liu, and L. Zhang, "Optimal generator start-up strategy for bulk power system restoration," *IEEE Transactions on Power Systems*, vol. 26, no. 3, pp. 1357–1366, 2011.

[11] Y. Jiang, S. Chen, C.-C. Liu, W. Sun, X. Luo, S. Liu, N. Bhatt, S. Uppalapati, and D. Forcum, "Blackstart capability planning for power system restoration," *International Journal of Electrical Power & Energy Systems*, vol. 86, pp. 127–137, 2017.

[12] A. Castillo, "Microgrid provision of blackstart in disaster recovery for power system restoration," in *Smart Grid Communications, 2013 IEEE International Conference on*. IEEE, 2013, pp. 534–539.

[13] Y.-T. Chou, C.-W. Liu, Y.-J. Wang, C.-C. Wu, and C.-C. Lin, "Development of a black start decision supporting system for isolated power systems," *IEEE Transactions on Power Systems*, vol. 28, no. 3, pp. 2202–2210, 2013.

[14] C. Wang, V. Vittal, and K. Sun, "OBDD-based sectionalizing strategies for parallel power system restoration," *IEEE Transactions on Power Systems*, vol. 26, no. 3, pp. 1426–1433, 2011.

[15] A. Golshani, W. Sun, Q. Zhou, Q. P. Zheng, and Y. Hou, "Incorporating wind energy in power system restoration planning," *IEEE Transactions on Smart Grid*, 2017.

[16] L. Yutian, F. Rui, and V. Terzija, "Power system restoration: a literature review from 2006 to 2016," *Journal of Modern Power Systems and Clean Energy*, vol. 4, no. 3, pp. 332–341, 2016.

[17] A. Castillo, "Risk analysis and management in power outage and restoration: A literature survey," *Electric Power Systems Research*, vol. 107, pp. 9–15, 2014.

[18] N. Saraf, K. McIntyre, J. Dumas, and S. Santoso, "The annual black start service selection analysis of ERCOT grid," *IEEE Transactions on Power Systems*, vol. 24, no. 4, pp. 1867–1874, 2009.

[19] W. Sun, C.-C. Liu, and S. Liu, "Black start capability assessment in power system restoration," in *Power and Energy Society General Meeting, 2011 IEEE*. IEEE, 2011, pp. 1–7.

[20] R. Kafka, "Review of PJM restoration practices and NERC restoration standards," in *Power and Energy Society General Meeting-Conversion and Delivery of Electrical Energy in the 21st Century, 2008 IEEE*. IEEE, 2008, pp. 1–5.

[21] *PJM Manual: System Restoration*, PJM, 6 2017, rev. 24.

[22] F. Qiu, J. Wang, C. Chen, and J. Tong, "Optimal black start resource allocation," *IEEE Transactions on Power Systems*, vol. 31, no. 3, pp. 2493–2494, 2016.

[23] F. Qiu and P. Li, "An integrated approach for power system restoration planning," *Proceedings of the IEEE*, 2017.

[24] C. Coffrin and P. Van Hentenryck, "Transmission system restoration with co-optimization of repairs, load pickups, and generation dispatch," *International Journal of Electrical Power & Energy Systems*, vol. 72, pp. 144–154, 2015.

[25] K. P. Schneider, E. Sortomme, S. Venkata, M. T. Miller, and L. Ponder, "Evaluating the magnitude and duration of cold load pick-up on residential distribution using multi-state load models," *IEEE Transactions on Power Systems*, vol. 31, no. 5, pp. 3765–3774, 2016.

[26] Z. Qin, Y. Hou, C.-C. Liu, S. Liu, and W. Sun, "Coordinating generation and load pickup during load restoration with discrete load increments and reserve constraints," *IET Generation, Transmission & Distribution*, vol. 9, no. 15, pp. 2437–2446, 2015.

[27] A. Gholami and F. Aminifar, "A hierarchical response-based approach to the load restoration problem," *IEEE Transactions on Smart Grid*, vol. 8, no. 4, pp. 1700–1709, 2017.

[28] W. Liu, Z. Lin, F. Wen, and G. Ledwich, "A wide area monitoring system based load restoration method," *IEEE Transactions on Power Systems*, vol. 28, no. 2, pp. 2025–2034, 2013.

[29] S. Liao, W. Yao, X. Han, J. Wen, and Y. Hou, "Two-stage optimization method for network reconfiguration and load recovery during power system restoration," in *Power & Energy Society General Meeting, 2015 IEEE*. IEEE, 2015, pp. 1–5.

[30] K. W. Hedman, R. P. O'Neill, E. B. Fisher, and S. S. Oren, "Optimal transmission switching with contingency analysis," *IEEE Transactions on Power Systems*, vol. 24, no. 3, pp. 1577–1586, 2009.

[31] P. A. Trodden, W. A. Bukhsh, A. Grothey, and K. I. McKinnon, "Optimization-based islanding of power networks using piecewise linear ac power flow," *IEEE Transactions on Power Systems*, vol. 29, no. 3, pp. 1212–1220, 2014.

[32] C. Guéret, C. Prins, and M. Sevaux, "Applications of optimization with Xpress-MP," *contract*, p. 00034, 1999.

[33] T. Athay, R. Podmore, and S. Virmani, "A practical method for the direct analysis of transient stability," *IEEE Transactions on Power Apparatus and Systems*, no. 2, pp. 573–584, 1979.

[34] R. D. Zimmerman, "MATPOWER 4.0 b4 Users manual," *Power Syst Eng Res Cent*, pp. 1–105, 2010.

[35] D. Wang, X. Gu, G. Zhou, S. Li, and H. Liang, "Decision-making optimization of power system extended black-start coordinating unit restoration with load restoration," *International Transactions on Electrical Energy Systems*, 2017.

[36] N.-P. Yu, C.-C. Liu, and J. Price, "Evaluation of market rules using a multi-agent system method," *IEEE Transactions on Power Systems*, vol. 25, no. 1, pp. 470–479, 2010.

[37] A. Papavasiliou, S. S. Oren, and R. P. O'Neill, "Reserve requirements for wind power integration: A scenario-based stochastic programming framework," *IEEE Transactions on Power Systems*, vol. 26, no. 4, pp. 2197–2206, 2011.

[38] K. P. Schneider, F. K. Tuffner, M. A. Elizondo, C.-C. Liu, Y. Xu, and D. Ton, "Evaluating the feasibility to use microgrids as a resiliency resource," *IEEE Transactions on Smart Grid*, vol. 8, no. 2, pp. 687–696, 2017.

Georgios Patsakis (S'12) received his B.Sc. degree with highest distinction in electrical and computer engineering from the National Technical University of Athens (NTUA), Greece, in 2013. He received his M.Sc. degree in industrial engineering and operations research (IEOR) from the University of California, Berkeley, USA in 2016, where he is currently pursuing a Ph.D. degree. His current research interests include optimization for power systems applications with a focus on Mixed Integer Programming. He has also worked on control for power electronics and electric drives, as well as on wind turbine and HVDC modeling and control. He has received the IEOR Faculty Fellowship Award at UC Berkeley in 2017, the Chrysovergeio Award at NTUA in 2013, and he is a Fellow of the Onassis Foundation.

Deepak Rajan is an Associate Adjunct Professor of Industrial Engineering and Operations Research at the University of California at Berkeley. Dr. Rajan is the author of more than 30 technical publications and 10 patents. He earned his M.S. and Ph.D. in Operations Research from the University of California at Berkeley, and also holds a B.Tech. from the Indian Institute of Technology at Madras, with a major in Mechanical Engineering. Following graduate school, Dr. Rajan completed a post-doctoral year at IBM T.J. Watson Research Center, and then worked as a Research Staff Member at IBM T.J. Watson Research Center since 2005. Since 2011, he has been working at Lawrence Livermore National Laboratory, where he focuses on developing algorithms and software using computational optimization techniques, and leading/contributing to projects that leverage such techniques.

Ignacio Aravena (S'13) obtained his B.Sc. and M.Sc. degrees in electrical engineering from Universidad Tcnica Federico Santa Mara, Chile, where he also served as lecturer and as industrial consultant. He is currently a Ph.D. student on Applied Mathematics at Universit catholique de Louvain (UCL), Belgium. His research interests include energy optimization, renewable energy integration in power systems, stochastic and robust programming, and distributed optimization.

Jennifer Rios holds a BSc degree in electrical engineering from San Francisco State University (CA). She has been with PG&E since 1996, where she currently manages PG&E's Electric System Restoration Guidelines, the AGORA Advance Applications/System Restoration Tool and provides training and real-time support to system dispatchers.

Shmuel S. Oren (F'02-LF'15) received the B.Sc. and M.Sc. degrees in mechanical engineering and in materials engineering from the Technion Haifa, Haifa, Israel, and the M.S. and Ph.D. degrees in engineering economic systems from Stanford University, Stanford, CA, USA. He is the Earl J. Isaac Chair Professor in the Department of Industrial Engineering and Operations Research, University of California, Berkeley, CA, USA. He is the Berkeley Site Director in the Power System Engineering Research Center and former member of the Market Surveillance Committee of the California ISO. He has published numerous articles on aspects of electricity market design and has been a consultant to various private and government organizations. Dr. Oren is a member of the NAE and a Fellow of INFORMS.